

Möbius Domain-Wall fermions on gradient-flowed dynamical HISQ ensembles

Evan Berkowitz,^{1,2} Chris Bouchard,^{3,4} Chia Cheng Chang (張家丞),⁵ M. A. Clark,⁶
 Bálint Joó,⁷ Thorsten Kurth,⁸ Christopher Monahan,⁹ Amy Nicholson,^{10,5}
 Kostas Orginos,^{4,11} Enrico Rinaldi,^{12,2} Pavlos Vranas,^{2,5} and André Walker-Loud^{5,2}

¹*Institut für Kernphysik and Institute for Advanced Simulation, Forschungszentrum Jülich, 54245 Jülich Germany*

²*Nuclear and Chemical Sciences Division, Lawrence Livermore National Laboratory, Livermore, CA 94550, USA*

³*School of Physics and Astronomy, University of Glasgow, Glasgow G12 8QQ, UK*

⁴*Department of Physics, The College of William & Mary, Williamsburg, VA 23187, USA*

⁵*Nuclear Science Division, Lawrence Berkeley National Laboratory, Berkeley, CA 94720, USA*

⁶*NVIDIA Corporation, 2701 San Tomas Expressway, Santa Clara, CA 95050, USA*

⁷*Scientific Computing Group, Thomas Jefferson National Accelerator Facility, Newport News, VA 23606, USA*

⁸*NERSC, Lawrence Berkeley National Laboratory, Berkeley, CA 94720, USA*

⁹*New High Energy Theory Center and Department of Physics and Astronomy,
Rutgers, The State University of New Jersey, Piscataway, NJ 08854, USA*

¹⁰*Department of Physics, University of California, Berkeley, CA 94720, USA*

¹¹*Theory Center, Thomas Jefferson National Accelerator Facility, Newport News, VA 23606, USA*

¹²*RIKEN-BNL Research Center, Brookhaven National Laboratory, Upton, NY 11973, USA*

We report on salient features of a mixed lattice QCD action using valence Möbius Domain-Wall fermions solved on the dynamical $N_f = 2 + 1 + 1$ HISQ sea-quark ensembles generated by the MILC Collaboration. The approximate chiral symmetry properties of the valence fermions are shown to be significantly improved by utilizing the gradient-flow scheme to first smear the HISQ configurations. The greater numerical cost of the Möbius Domain-Wall inversions is mitigated by the highly efficient QUDA library optimized for NVIDIA GPU accelerated compute nodes. We provide tuned parameters of the action and performance of QUDA using ensembles with the lattice spacings $a \simeq \{0.15, 0.12, 0.09\}$ fm and pion masses $m_\pi \simeq \{310, 220, 135\}$ MeV. With a fixed flow time of $t_{gf} = 1$ in lattice units, the residual chiral symmetry breaking of the valence fermions is kept below 10% of the light quark mass on all ensembles, $m_{res} \lesssim 0.1 \times m_l$, with moderate values of the fifth dimension L_5 and a domain-wall height $M_5 \leq 1.3$.

I. INTRODUCTION

QCD (Quantum Chromodynamics) [1, 2] is the fundamental theory of the strong interaction, and one of the three gauge theories of the SM (Standard Model) of particle physics. QCD encodes the interactions between quarks and gluons, the constituents of strongly interacting matter, which both carry *color charges* of QCD. At short distances, the quarks and gluons perturbatively interact with a coupling strength that runs to zero in the UV (ultraviolet) limit [3, 4]. Conversely, at long-distance/low-energy, the IR (infrared) regime, the coupling becomes $\mathcal{O}(1)$ and QCD becomes a strongly coupled theory. Consequently, the quarks and gluons are confined into the *colorless* hadrons we observe in nature, such as the proton, neutron, pions, etc. In order to compute properties of nucleons, nuclei and other strongly interacting matter directly from QCD, we must therefore use a non-perturbative regularization scheme.

Asymptotic freedom, the property in which the gauge coupling becomes perturbative in the UV, makes the theory perfectly amenable to a numerical approach. QCD can be constructed on a discrete, Euclidean spacetime lattice, with a technique known as LQCD (lattice QCD). As the discretization scale is made sufficiently fine and the coupling becomes perturbative, the lattice action can be matched onto the continuum action to a desired order in perturbation theory. To aid the matching, EFT

(Effective Field Theory) [5] can be used to perform an expansion of the lattice action in powers of the discretization scale, typically denoted a , which is referred to as the Symanzik expansion [6, 7]. There are many different choices for constructing the discretized action, each of which corresponds to a different lattice action. As the continuum limit is taken, the difference between these lattice actions vanishes as the only dimension-4 operators allowed by the symmetries of all LQCD actions are exactly those of QCD: the discretization effects, which include Lorentz violating interactions, are all described by *irrelevant* operators in the Symanzik expansion. An important test of this universality is to perform calculations of various physical quantities, with different lattice actions, and show consistency between them in the continuum limit. This is now routinely done for mesonic quantities and reviewed every 2-3 years by the FLAG Working Group, with the latest review in Ref. [8].

Lattice gauge theory began with the formulation of gauge fields on a spacetime lattice as originally proposed by Wilson [9]. The inclusion of fermions presents further challenges. The *naive* discretization of the fermion action leads to the fermion doubling problem, in which there are 2^D fermions in D dimensions for each fermion field implemented. These doublers arise from the periodicity of the lattice action in momentum space and the single derivative in the Dirac equation. Wilson proposed the original method, now known as the Wilson fermion

action, to remove these doublers by adding an irrelevant operator to the action which provides an additive mass to the doublers which scales as $1/a$. This irrelevant operator breaks chiral symmetry and requires fine-tuning the bare fermion mass to simulate a theory with light fermions, such as QCD with light *up* and *down* quarks. Despite (or because of) its simplicity, the Wilson fermion action is still one of the most popular in use. These days, the leading $\mathcal{O}(a)$ discretization corrections are removed perturbatively or non-perturbatively through an additional dimension 5 operator, the clover operator $c_{SW} a \bar{q} \sigma_{\mu\nu} G_{\mu\nu} q$, in what is known as the Wilson-Clover or *Clover* fermion action. The parameter c_{SW} is the Sheikholeslami-Wohlert coefficient [10] which can be tuned to remove the $\mathcal{O}(a)$ discretization effects from correlation functions. The idea has also been extended to twisted mass Wilson fermions [11], in which a complex quark mass term is used allowing for automatic $\mathcal{O}(a)$ improvement of physical observables provided the theory is computed at *maximal twist* [12].

Another common lattice action is known as the Kogut-Susskind or *staggered* fermion action [13, 14]. This action reduces the number of fermion doublers by exploiting a symmetry of the *naive* fermion action. A suitable spacetime-dependent phase rotation of the fermion fields allows for the Dirac equation to be diagonalized, thereby reducing the number of doublers from 16 to 4, in 4 spacetime dimensions. To perform numerical simulations with just one or two light fermion flavors, a quarter or square root of the fermion determinant is used [15]. This rooting leads to non-local interactions at finite lattice spacing [16–18], however, perturbation theory [19, 20], the renormalization group [21–23] and numerical simulations [24–26] have been used to argue that these non-local effects vanish in the continuum limit. While this can not be proved non-perturbatively, some of the potential sicknesses of the theory can be shown to be the same as those of *partially quenched* lattice QCD [27], which we will discuss briefly in short order. While not universally accepted, all numerical evidence suggests that rooted-staggered LQCD is in the same universality class as QCD as the continuum limit is taken [8, 28–30].

Determining a non-perturbative regulator that both preserves chiral symmetry and has the correct number of light degrees of freedom is challenging. It has been shown that in 4 spacetime dimensions, one can not simultaneously have all four of the conditions: chiral symmetry, ultra local action, undoubled fermions and the correct continuum limit. This is known as the Nielson-Ninomiya no-go theorem [31–33]. However, one can extend the definition of chiral symmetry at finite lattice spacing: if the lattice Dirac operator, D , satisfies the Ginsparg-Wilson relation [34]

$$\{\gamma_5, D\} = aD\gamma_5 D, \quad (1)$$

it will respect chiral symmetry even at finite lattice spacing [35]. One consequence is the theory will be automatically $\mathcal{O}(a)$ improved as the only non-trivial dimension-

5 operator that can not be removed through field redefinitions and equations of motion is the clover operator, which explicitly breaks chiral symmetry, and is thus not allowed. There are two lattice actions which satisfy the Ginsparg-Wilson relation: the DW (domain-wall) fermion action [36–38] and the overlap fermion action [39–41]. The DW fermion action is formulated with a finite fifth dimension of extent L_5 , where the left and right chiral modes are bound to opposite ends of the fifth dimension. The gluon action is a trivial copy of the 4D action on each fifth dimensional slice with unit link variable between the slices and so the fermions have only a simple kinetic action in the fifth dimension. At finite L_5 the left and right modes have a non-vanishing overlap due to fermion modes which propagate into the fifth dimension. The massive modes decay exponentially in the fifth dimension while the fermion zero modes have only a power-law fall off. This small overlap leads to a small, residual breaking of chiral symmetry at finite L_5 , characterized by a quantity known as m_{res} . The overlap fermion action can be shown to be equivalent to the domain-wall action as $L_5 \rightarrow \infty$ [42, 43], and respects chiral symmetry to a desired numerical precision.

The numerical cost of generating lattice ensembles with domain-wall and overlap actions is one or more orders of magnitude greater than the cost of generating ensembles with Wilson-type or staggered fermion actions [44]. This has led to interest in, and the development of, mixed lattice actions or MA (mixed-actions) [45], in which the valence and sea quark lattice actions are not the same at finite lattice spacing. In the most common MALQCD calculations, the dynamical sea-quark action is generated with a numerically less expensive discretization scheme, such as staggered- or Wilson-type fermions, while the valence-quark action, which is used to construct correlation functions, is implemented with domain-wall or overlap fermions, thus retaining the full chiral symmetry in the valence sector. The first implementation of a MALQCD calculation was performed by the LHP Collaboration [46] utilizing DW fermions on the publicly available asqtad (a^2 tadpole improved) [47, 48] rooted staggered ensembles generated by the MILC Collaboration [30, 49]. A number of important results were obtained with this particular MALQCD setup, including the first dynamical calculation of the nucleon axial charge with light pion masses [50] and more general nucleon structure [51, 52], the first dynamical calculation of two-nucleon elastic scattering [53], a precise calculation of the $I = 2 \pi\pi$ scattering length [54], a detailed study of the quark mass dependence of the light baryon spectrum [55], a calculation of the kaon bag parameter with fully controlled uncertainties [56] and many more.

The predominant reason for the success of these MALQCD calculations is the good chiral symmetry properties of the DW action, which significantly suppresses chiral symmetry breaking from the staggered sea fermions and discretization effects. EFT can be used to

understand the salient features of such MALQCD calculations. χ PT (Chiral Perturbation Theory) [57–59] can be extended to incorporate discretization effects into the analytic formulae describing the quark mass dependence of various hadronic quantities. The procedure is to first construct the local Symanzik Action for a given lattice action, and then to use spurion analysis to construct all operators in the low-energy EFT describing such a lattice action, including contributions from higher dimension operators [60]. The MAEFT [61] for DW valence fermions on dynamical rooted staggered fermions is well developed [62–69]. The use of valence fermions which respect chiral symmetry leads to a universal form of the MAEFT extrapolation formulae at NLO (next-to-leading order) in the dual quark-mass and lattice spacing expansions [65, 68]. This universal behavior follows from the suppression of chiral symmetry breaking discretization effects from the sea sector when constructing correlation functions from valence fermions. Further, quantities which are protected by chiral symmetry are free of new LECs (low-energy constants) at NLO provided on-shell renormalized quantities are used in the extrapolation formulae [64, 65]. This universality allows for the derivation of NLO MAEFT formula directly from their PQ χ PT (partially quenched χ PT) [70–78] counterparts, provided they are known [79–86]. MALQCD calculations with DW valence quarks on the asqtad rooted staggered ensembles have been stress-tested through a comparison of quantities which are directly sensitive to the unitarity violations present in MALQCD calculations, in particular the a_0 meson correlation function [87, 88].

There are a few other MA constructions that have been tested, but only three others that are actively used. The HPQCD Collaboration utilizes HISQ valence fermions on the asqtad ensembles, for example, see Refs. [89, 90]. The χ QCD Collaboration utilizes overlap valence fermions on the dynamical $N_f = 2 + 1$ domain-wall ensembles [91–93] generated by the RBC/UKQCD Collaboration [94, 95]. The PNDME Collaboration has utilized clover improved valence fermions on the $N_f = 2 + 1 + 1$ HISQ ensembles [96]. While this MA choice is economical, it does not benefit from the suppression of chiral symmetry breaking discretization effects as with the DW on asqtad or overlap on DW MALQCD calculations, and this is observed in the size of the discretization effects present in the calculations [97].

Given the successes described above, MALQCD provides an economical means of performing LQCD calculations in which chiral symmetry breaking effects are highly suppressed by utilizing a valence fermion action that respects chiral symmetry in combination with a set of LQCD ensembles that do not, but are less numerically expensive to generate. In this article, we motivate a new MALQCD action and present numerical evidence for salient features of the action.

II. MÖBIUS DOMAIN-WALL FERMIONS ON GRADIENT-FLOWED HISQ ENSEMBLES

Present day LQCD calculations for mesonic quantities are performed with multiple lattice spacings, multiple volumes and physical pion masses, allowing for complete control over all LQCD systematics, see Ref. [8] for many examples. The simplest single baryon properties are also computed with multiple lattice spacings/volumes and near-physical and sometimes physical pion masses [98–101], including the first calculation of the nucleon axial charge with both physical pion masses and a continuum limit [102] and isospin violating corrections [102–105]. If one is interested in a set of ensembles allowing for this much control over LQCD systematics, there are only two such sets publicly available, both of which are generated and provided by the MILC Collaboration: the $N_f = 2 + 1$ asqtad ensembles [30] and the $N_f = 2 + 1 + 1$ HISQ (highly improved staggered quark) [106] ensembles generated more recently [107]. The HISQ ensembles have taste-splittings in the pseudoscalar sector that are one generation finer in discretization [107], such that the $a \sim 0.15$ fm HISQ ensemble taste violations are similar in size to the $a \sim 0.12$ fm asqtad ensembles. There is a vast set of HISQ ensembles with $130 \lesssim m_\pi \lesssim 310$ MeV, strange and charm quark masses tuned near their physical values and lattice spacings of $a \sim \{0.15, 0.12, 0.09, 0.06, 0.042, 0.03\}$ fm, including multiple spatial volumes and lighter than physical strange quark masses. In Table I, we list the HISQ ensembles utilized in the present work as well as ensembles for which we have tuned the MDWF parameters for future work.

Given the great success of the MA DW fermion on asqtad LQCD calculations [51–53, 55, 56, 108, 109], we have chosen to use DW fermions for the present MALQCD calculations as well. In the present work, we have chosen to use the MDWF (Möbius DW fermion) action [110–112] which offers reduced residual chiral symmetry breaking at fixed fifth dimensional extent, L_5 . With the introduction of two new parameters, b_5 and c_5 , the Möbius kernel can be smoothly interpolated between the Shamir [37] and the Neuberger/Boriçi [42, 43, 113, 114] kernels. Following Ref. [112], the Möbius kernel can be expressed

$$D^{\text{Möbius}}(M_5) = \frac{(b_5 + c_5)D^{\text{Wilson}}(M_5)}{2 + (b_5 - c_5)D^{\text{Wilson}}(M_5)}. \quad (2)$$

Alternatives include a polar decomposition to the sign function [115–117] or other methods of approximating the sign function [118]. In this work, we have always chosen values of b_5 and c_5 with the constraint $b_5 - c_5 = 1$, such that the Möbius kernel is a rescaled version of the Shamir kernel

$$D^{\text{Möbius}}(M_5) = \frac{\alpha D^{\text{Wilson}}(M_5)}{2 + D^{\text{Wilson}}(M_5)} \equiv \alpha D^{\text{Shamir}}(M_5). \quad (3)$$

It was demonstrated in Ref. [112] that this rescaling factor, α , exponentially enhances the suppression of residual

short name	ensemble	am_π^{HISQ-5}	am_{ss}^{HISQ-5}	volume	$\sim a$ [fm]	$\sim m_\pi$ [MeV]	$m_\pi L$	N_{cfg}	$\Delta\tau_{MC}$
a15m310	l1648f211b580m013m065m838a	0.23646(17)	0.51858(17)	$16^3 \times 48$	0.15	310	3.78	196	50
a12m310	l2464f211b600m0102m0509m635a	0.18931(10)	0.41818(10)	$24^3 \times 64$	0.12	310	4.54	199	25
a09m310	l3296f211b630m0074m037m440e	0.14066(13)	0.31133(12)	$32^3 \times 96$	0.09	310	4.50	196	24
a15m220	l2448f211b580m0064m0640m828a	0.16612(08)	0.51237(10)	$24^3 \times 48$	0.15	220	3.99	199	25
a12m220	l3264f211b600m00507m0507m628a	0.13407(06)	0.41559(07)	$32^3 \times 64$	0.12	220	4.29	199	25
a09m220	l4896f211b630m00363m0363m430a	0.09849(07)	0.30667(07)	$48^3 \times 96$	0.09	220	4.73	—	—
a15m130	l3248f211b580m00235m0647m831a	0.10161(06)	0.51427(05)	$32^3 \times 48$	0.15	130	3.25	—	—
a12m135	l4864f211b600m00184m0507m628a	0.08153(04)	0.41475(05)	$48^3 \times 64$	0.12	135	3.91	—	—

TABLE I. The HISQ ensembles used in this work and planned for future MALQCD calculations. In addition to the pion mass and lattice spacing, we list the number of configurations used in the present work, N_{cfg} as well as the Monte-Carlo time, $\Delta\tau_{MC}$, by which the configurations were separated in this work. The short name, introduced in Ref. [97], is for brevity.

chiral symmetry breaking as

$$m_{res} \sim e^{-\alpha L_5}, \quad (4)$$

provided the action is in a regime where these exponentially damped terms are the dominant contribution to m_{res} and α is not too large, but of the order $\alpha \sim 2 - 4$. With the constraint $b_5 - c_5 = 1$, the rescaling factor is given by $\alpha = b_5 + c_5$.

A. Gradient-flow smearing

From the DW on asqtad action [108], it is known that the asqtad gauge fields required additional levels of smearing to reduce the residual chiral symmetry breaking. For that action, HYP smearing [119–122] was utilized for this purpose. In this work, we choose to investigate the use of the gradient flow [123–125] as a smearing method. The gradient flow is a nonperturbative, classical evolution of the original fields in a new parameter, the *flow time*, that drives those fields towards a classical minimum. In real space, this corresponds to smearing out the degrees of freedom through an infinitesimal *stout-smearing* procedure [126].

Gradient flow smearing introduces a new scale, of the order $l_{gf} \sim \sqrt{8t_{gf}}a$, where t_{gf} is the (dimensionless) flow time. Correlation functions depend upon this new scale, which can serve as a nonperturbative, rotationally-invariant UV regulator that provides the possibility for improved renormalization procedures for various LQCD matrix elements [127–133]. Here, however, we are interested in the gradient flow as a smearing algorithm [134, 135].

To ensure that the continuum limit of LQCD matrix elements is free of any flow time dependence, one must use a fixed flow time in lattice units such that all flow time dependence extrapolates to zero as the continuum limit is taken.

In this work, we have found that moderate values of the flow time allow for a reduction of the residual chiral

symmetry breaking such that $m_{res} < 0.1 \times m_l^{dwf}$ for moderate values of L_5 . The resulting flow time dependence of m_{res} at fixed pion mass demonstrates that the gradient flow highly suppresses the zero-mode contributions to m_{res} , such that an exponential dependence of m_{res} on L_5 is recovered. Further, we have observed that gradient flow smearing has allowed us to use small values of the DW height, with $M_5 \leq 1.3$ on all ensembles used in this work. This is important because with the larger values of M_5 used in the DW on asqtad calculations, there was strong contamination of the UV modes with an oscillatory time behavior, modes which are known to decouple as $M_5 \rightarrow 1$ [136]. With the values of M_5 used in this work, there is no discernable contamination from these modes at larger flow times.

We finally settled on a gradient flow time of $t_{gf} = 1.0$, which provided significant suppression of residual chiral symmetry breaking without introducing a large flow time length scale. In the next section, we present detailed calculations showing the flow time dependence of various quantities. This action has been used to compute the $\pi^- \rightarrow \pi^+$ matrix element relevant for neutrinoless double beta-decay [137] and also to perform an exploratory calculation of an improved method of computing hadronic matrix elements [138].

III. TUNING THE ACTION

With a given flow time, our general algorithm for choosing values of the MDWF action parameters is to:

1. For a fixed value of L_5 , optimize M_5 to minimize the resulting value of m_{res} ;
2. Vary the values of L_5 , b_5 and c_5 under the constraints $b_5 - c_5 = 1$ and $m_{res} \leq 0.1m_l^{dwf}$ while minimizing L_5 ;
3. Tune m_l^{dwf} and m_s^{dwf} such that $m_l^{dwf} \simeq m_\pi^{HISQ-5}$ and $m_s^{dwf} \simeq m_{ss}^{HISQ-5}$ within $\mathcal{O}(2\%)$ or less where

HISQ–5 denotes the taste-5 pseudoscalar mass of the dynamical HISQ action and m_{ss} is the mass of the connected $\bar{s}\gamma_5 s$ pseudoscalar meson.

This procedure required just a few iterations to converge to the desired results. For this work, we have used the definition of m_{res} from the Shamir kernel as the residual chiral symmetry breaking between Shamir and Möbius become the same in the continuum limit [112],

$$m_{res}(t) = \frac{\sum_{\mathbf{x}} \langle \bar{Q}(t, \mathbf{x}) \gamma_5 Q(t, \mathbf{x}) \bar{q}(0, \mathbf{0}) \gamma_5 q(0, \mathbf{0}) \rangle}{\sum_{\mathbf{x}} \langle \bar{q}(t, \mathbf{x}) \gamma_5 q(t, \mathbf{x}) \bar{q}(0, \mathbf{0}) \gamma_5 q(0, \mathbf{0}) \rangle}, \quad (5)$$

where Q is a quark field in the midpoint of the 5th dimension and q is a quark field bound to the domain-wall.

A. Flow time dependence of various quantities and the continuum limit

To study the efficacy of this action, we compute the flow time dependence of various quantities and show that the continuum limits of various ratios of physical quantities are flow time independent. In order to test the flow time dependence, we tune the input quark masses to hold the pion mass and the connected $\bar{s}s$ pseudoscalar meson masses fixed within $\mathcal{O}(2\%)$. In the appendix (Table VI), we list the tuned values of the input quark masses for various flow times on the ensembles used in this work. In Figure 1, we show the effective masses of the pion and nucleon, respectively, on the a15m310 ensemble for all flow times. We observe that the contamination from oscillatory modes are suppressed at larger flow times.

From the input quark masses used at fixed pseudoscalar masses, and the average values of the plaquettes, one can observe a substantial flow time dependence of UV quantities. This is expected as the gradient flow smearing filters out the UV modes of the gauge fields. It is important to check the flow time dependence of hadronic quantities, including the continuum limit of ratios of hadronic quantities are flow time independent. In Table VII, we list values of F_π , F_K , m_N and the quark-mass dependent axial renormalization constants determined on the various ensembles at different flow times. We also list the ratios of F_K/F_π and m_N/F_π . In order to determine the pseudoscalar decay constants, we utilize the 5D Ward Identity relating the renormalized decay constants to various correlation functions including those used to determine the values of m_{res} [139, 140],

$$F_{q_1 q_2} = \frac{A_{PS}}{\sqrt{A_{SS}}} \frac{m_{q_1} + m_{q_1}^{res} + m_{q_2} + m_{q_2}^{res}}{m_{1,2}^{3/2}}, \quad (6)$$

where $A_{PS} = Z_P Z_S$ is the combined overlap factor of the ground state point-sink smeared-source pseudoscalar two-point function and A_{SS} is similarly the overlap factor for a smeared-sink and smeared-source. The pseudoscalar meson mass composed of quarks q_1 and q_2 is

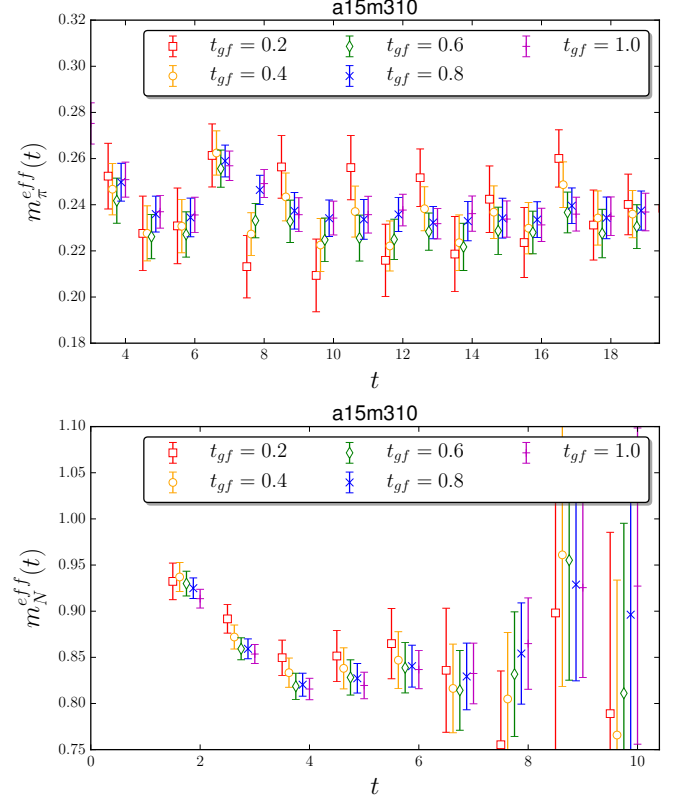


FIG. 1. Effective mass of the pion (top) and proton (bottom) as a function of the Euclidean time t , at different flow times on the a15m310 ensemble. The different flow time values are slightly shifted horizontally for visual clarity.

given by $m_{1,2}$. This normalization is such that the physical pion decay constant is $F_\pi = 92.2$ MeV.

In order to determine the axial renormalization constants, we can also compute the bare values of $F_{q_1 q_2}$ using the 4D axial-vector current, e.g. for the pion

$$\begin{aligned} \partial_4 \langle 0 | A_4(t) P_S(0) | 0 \rangle &= -\langle 0 | A_4 | \pi \rangle Z_S m_\pi e^{-m_\pi t} + \dots \\ &= \frac{F_\pi}{Z_A} Z_S m_\pi^{3/2} e^{-m_\pi t} + \dots \end{aligned} \quad (7)$$

where the \dots denote the wrap-around contributions ($e^{-m_\pi(T-t)}$) and excited state contributions (normal and oscillating) to the correlation function and Z_S is the same ground state overlap factor determined in the two-point function.

1. Observations about flow time dependence

From our calculations, there are a few substantial benefits one observes from use of the gradient flow smearing. Before discussing these, we first comment on the strong oscillations observed at small flow time dependence in the pseudoscalar correlators. In Figure 1, we observe a strong signal for an oscillating excited state with $(-1)^t$ behavior (where t is the Euclidean time) at small flow times,

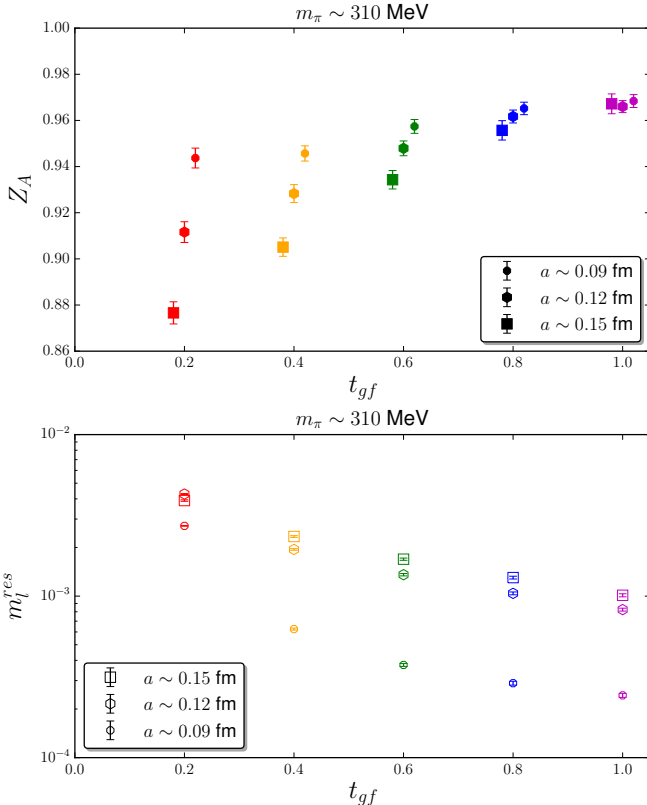


FIG. 2. Z_A (top) and m_l^{res} (bottom) as a function of flow time on the $m_\pi \simeq 310$ MeV ensembles. The results of Z_A are slightly shifted horizontally for visual clarity.

most notably for $t_{gf} = 0.2$. These oscillating modes become completely damped out for $t_{gf} \geq 0.6$, with the statistics used in this work. For the smaller flow times, these oscillations lead to additional fitting systematics. However, these additional systematics will only further contribute to the consistency of the various flow times through increased total uncertainties of the small flow time numerical results. In this work, the comparison of results for different flow times includes only stochastic uncertainties. To ensure we retain the maximum correlation between quantities computed at different flow times, we restrict the fits of the two-point and 4D axial-vector current correlation functions to reside on the same time window on a given ensemble for each flow time. We further set $t_{\min} = 0.6$ fm for the $a \sim 0.15$ fm and $a \sim 0.12$ fm ensembles and $t_{\min} = 0.9$ fm for the $a \sim 0.09$ fm ensemble to minimize systematic fluctuations introduced by a choice of fit window.

The first significant benefit observed is that as the flow time is increased, a dramatic reduction of the chiral symmetry breaking properties of the valence MDWF action is achieved. This can be observed in the significant reduction in m_{res} at fixed pion mass or similarly, the values of Z_A approaching 1 for all gauge couplings, both of which are depicted in Figure 2. At $t_{gf} = 1$, the value of Z_A becomes effectively independent of the lattice spacing, and

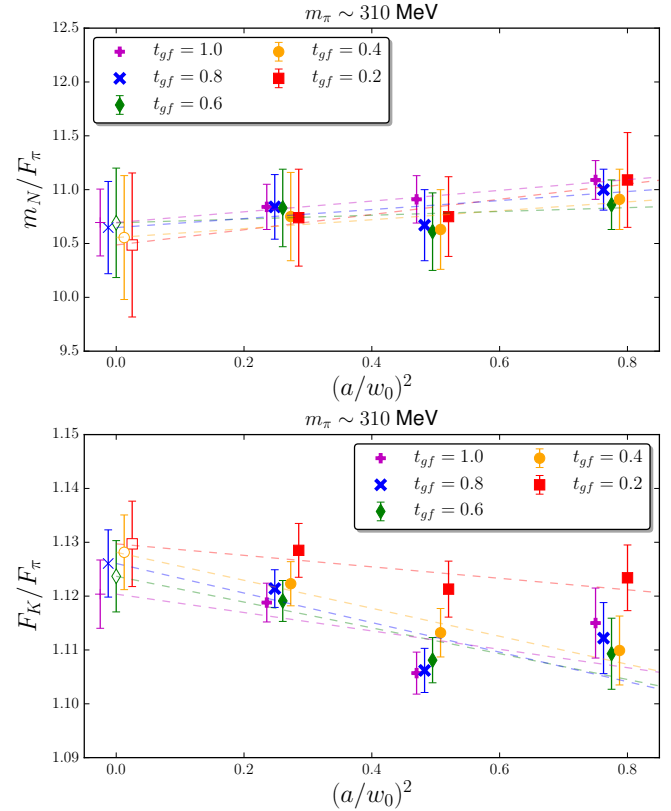


FIG. 3. Flow time (in)dependence of m_N/F_π and F_K/F_π on the $m_\pi \sim 310$ MeV ensembles. The filled in symbols are the results of our calculations and the open symbols clustered at $a/w_0 = 0$ are the continuum extrapolated results using the simple ansatz of a constant plus $(a/w_0)^2$ term. The results are slightly shifted horizontally for visual clarity.

close to 1. With the tuning we have chosen, to hold the pion mass, as well as L_5 , M_5 , b_5 and c_5 , fixed as we vary the flow time, we observe an exponential reduction in m_{res} as the flow time is increased. Though not depicted in these figures or tables, we also studied the dependence of m_{res} on L_5 as the flow time was varied. We find that for small flow time, the reduction in m_{res} as L_5 increases is power-law, indicating the 5D zero-mode contributions are dominating the residual chiral symmetry breaking. As we increase the flow time, m_{res} begins to fall off exponentially in L_5 , indicating the gradient flow smearing suppresses these zero-mode contributions.

Another significant benefit we observe is that stochastic fluctuations become smaller for increasing flow time. This is observed from the sample effective mass plots of the nucleon and pion in Figure 1. The gradient flow is applied in all 4 spacetime directions, so the neighboring time slices become more correlated, rendering a direct comparison of the effective mass plots more complicated. However, the list of fitted quantities in Table VII demonstrates the correlated stochastic uncertainties are reduced for increasing flow time. Comparing the $t_{gf} = 1$ to $t_{gf} = 0.2$ results, we observe approximately a factor of

$\sqrt{2}$ reduction the stochastic uncertainty for equal computing cost.

In Figure 3, we show a continuum study of m_N/F_π and F_K/F_π on the $m_\pi \sim 310$ MeV ensembles, for all flow times used. We explore four different continuum extrapolation ansätze for a quantity f :

$$f(a/w_0) = \begin{cases} f_0, & \text{constant ,} \\ f_0 + f_2 \frac{a^2}{w_0^2}, & \text{linear in } a^2 , \\ f_0 + \alpha_s f_2' \frac{a^2}{w_0^2}, & \text{linear in } \alpha_s a^2 , \\ f_0 + f_4 \frac{a^4}{w_0^4}, & \text{quadratic in } a^2 . \end{cases} \quad (8)$$

The gradient flow scale w_0 was first defined in Ref. [141], and a value of w_0 [141] = 0.1755(18)(04) fm was determined. The value determined in Ref. [142] is similar with a slight discrepancy, w_0 [142] = 0.1714(¹⁵)₍₁₂₎ fm. We use this value as we are using the same ensembles on which it was determined. With only three lattice spacings, we choose not to perform an extrapolation in both a^2 and either $\alpha_s a^2$ or a^4 simultaneously. However, we observe the value of f_2 for both m_N/F_π and F_K/F_π to be small and often consistent with zero. This motivates exploring the linear in $\alpha_s a^2$ and a^4 fits as estimates of systematic uncertainties in the continuum extrapolation. We find all four continuum extrapolations show consistency at the 1-sigma level both between all four different fit ansatz and also between the various flow time extrapolations. In Figure 3, we display the continuum extrapolation using the linear in $(a/w_0)^2$ ansatz. The quark-mass independent values of a/w_0 and α_s are taken from Ref. [142].

For m_N/F_π , we observe minimal discretization corrections with a slope in $(a/w_0)^2$ consistent with zero. For F_K/F_π , a quantity which is determined much more precisely for equal stochastic sampling, we observe mild, though still quite small, discretization corrections. While the discretization corrections are basically flow time independent for m_N/F_π , they seem to become more pronounced for F_K/F_π as the flow time is increased. There is an indication of the presence of higher order quartic in a/w_0 corrections, but we are not able to resolve these with the numerical results in this work. Previous studies of the heavy-light decay constants observed that large amounts of APE smearing [143] could induce significant higher order discretization effects [144]. It is possible that the larger t_{gf} smearings are having a similar effect on the strange quark, and thus the value of F_K , at the sub-percent level. These potential systematic uncertainties should be explored in more detail for a sub-percent calculation of F_K/F_π using this action.

B. Mixed-Meson mass corrections

In order to use the MAEFT extrapolation formulae, there are a few additional quantities which must be determined from the MALQCD calculations. At NLO in the MAEFT expansion, one needs to know the masses

of the mixed valence-sea mesons which propagate in virtual loops, and the value of the partial quenching parameter which controls the unitarity violating contributions [65, 68]. In a general MALQCD calculation with a chirally-symmetric valence action, one has

$$\begin{aligned} m_{vs}^2 &= \frac{1}{2} (m_{vv}^2 + m_{ss}^2) + a^2 \tilde{\Delta}_{\text{Mix}} , \\ \Delta_{\text{PQ}}^2 &= m_{ss}^2 - m_{vv}^2 , \end{aligned} \quad (9)$$

where m_{vv} is the mass of the pseudoscalar valence-valence meson, m_{ss} is the mass of the pseudoscalar sea-sea meson including possible additive discretization corrections, and $a^2 \tilde{\Delta}_{\text{Mix}}$ is an additional additive discretization correction to the mass of a meson composed of one valence and one sea quark. For our MALQCD calculations, these two quantities are given by [65, 68, 69]

$$\begin{aligned} m_{vs}^2 &= \frac{1}{2} (m_{vv}^2 + m_{ss,5}^2) + a^2 \tilde{\Delta}_{\text{Mix}} , \\ a^2 \tilde{\Delta}_{\text{Mix}} &= a^2 \Delta_{\text{Mix}} + \frac{a^2}{8} \Delta_A + \frac{3a^2}{16} \Delta_T + \frac{a^2}{8} \Delta_V + \frac{a^2}{32} \Delta_I , \\ a^2 \Delta_{\text{Mix}} &= \frac{8a^2 C_{\text{Mix}}}{F^2} , \\ \Delta_{\text{PQ}}^2 &= m_{ss,5}^2 + a^2 \Delta_I - m_{vv}^2 , \end{aligned} \quad (10)$$

where $m_{ss,5}$ is the mass of the taste-5 pseudoscalar meson, $a^2 \Delta_B$ are the taste splittings between the other taste-meson and the taste-5 meson, $a^2 \Delta_B = m_B^2 - m_5^2$, F is the leading order pion decay constant and C_{Mix} is the LEC of a new operator present in the MAEFT Lagrangian at $\mathcal{O}(a^2)$. The mixed-meson mass splitting, $a^2 \Delta_{\text{Mix}}$ is universal at LO in the MAEFT expansion [62], regardless of the taste of the staggered sea-quark partnered with the DW quark. In Ref. [66], it was observed that there is a noticeable quark mass dependence of the mixed-meson splitting, as defined e.g. for the pion

$$\Delta m_{vs}^2 \equiv m_{\pi,vs}^2 - \frac{1}{2} (m_{\pi,DW}^2 + m_{\pi,5}^2) . \quad (11)$$

There are three common methods of incorporating these discretization corrections:

1. power-series expand the discretization corrections about $a = 0$ and use a continuum EFT extrapolation enhanced by general corrections of the form $a^2, a^2 \alpha_S$, etc.;
2. extrapolate these mixed-meson discretization corrections to the chiral limit and use a uniform correction for all mixed-mesons with the full MAEFT expressions;
3. use the on-shell renormalized mixed-meson masses as they are on each ensemble with the full MAEFT expressions.

Provided the discretization corrections are under control, all three methods should agree in the continuum limit. It

ensemble	am_{uj}	am_{sj}	am_{ur}	am_{sr}
a15m310	0.300(6)	0.432(4)	0.444(5)	0.549(2)
a12m310	0.216(2)	0.334(2)	0.339(2)	0.430(1)
a09m310	0.150(1)	0.243(1)	0.247(1)	0.315(1)
a15m220	0.255(3)	0.416(3)	0.430(3)	0.543(1)
a12m220	0.178(2)	0.321(2)	0.335(2)	0.428(1)

TABLE II. The mixed-meson mass spectrum determined on ensembles used in this work, with flow time $t_{gf} = 1$.

is useful, therefore, to determine the mixed meson masses for all combinations of valence and sea quarks used in the MALQCD calculations.

In order to compute the mixed-meson spectrum, we need to construct pseudoscalar mesons composed of one MDWF and one HISQ fermion propagator. To compute the MDWF propagators, we have used the QUDA library interfaced from Chroma with solutions generated with gauge-covariant Gaussian smeared sources [145]. To compute the HISQ propagators, we utilized the MILC code. To minimize the gauge noise, we similarly used a gauge-covariant source for the staggered fermions. This source was created in Chroma, with routines added to the `devel` branch to support writing a source file readable as a `vector_field` source by the MILC code. The MDWF fermions were converted to the `DD_PAIRS` format to be read by MILC, which was used to compute the mixed-meson and HISQ-HISQ pseudoscalar spectrum. To further reduce the gauge noise, the mixed-meson correlation functions were constructed with interpolating operators

$$\mathcal{O}_{vs} = \bar{q}_{val}\gamma_5 q_{sea} \quad (12)$$

as well as their Hermitian conjugates. The real part of the averaged conjugate pairs of correlation functions were then used to determine the spectrum, which were computed with all possible pairings of light and strange quarks with one MDWF and one HISQ type quark propagator.

In Table II, we list the masses of mixed-mesons computed in this work, using only flow time $t_{gf} = 1$ ensembles. In Table III, we list the values of the splittings Δm_{vs}^2 , defined as in Eq. (11), and m_{vv} and m_{ss} are the pseudoscalar masses of the valence-valence and sea-sea mesons respectively. The values are listed in w_0 units where the quark-mass independent values w_0/a are taken from Ref. [142]. We use the notation of Ref. [73] and denote the various mixed-mesons as

$$\begin{aligned} \phi_{uj} &= \text{pion: val. light } u, \text{ sea light } j, \\ \phi_{ur} &= \text{kaon: val. light } u, \text{ sea strange } r, \\ \phi_{sj} &= \text{kaon: val. strange } s, \text{ sea light } j, \\ \phi_{sr} &= \bar{s}\gamma_5 s: \text{ val. strange } s, \text{ sea strange } r. \end{aligned} \quad (13)$$

ensemble	$w_0^2\Delta m_{uj}^2$	$w_0^2\Delta m_{sj}^2$	$w_0^2\Delta m_{ur}^2$	$w_0^2\Delta m_{sr}^2$
a15m310	0.0439(41)	0.0298(40)	0.0440(59)	0.0422(28)
a12m310	0.0214(17)	0.0123(29)	0.0199(30)	0.0206(22)
a09m310	0.0102(09)	0.0038(18)	0.0102(19)	0.0085(14)
a15m220	0.0488(38)	0.0341(58)	0.0488(60)	0.0410(36)
a12m220	0.0279(13)	0.0142(20)	0.0334(30)	0.0212(20)

TABLE III. The mixed-meson mass splittings (Eq. 11) determined on ensembles used in this work, with flow time $t_{gf} = 1$. The values of w_0/a are determined from Ref. [142].

ensemble	M_5	L_5	b_5	c_5	t_{gf}	am_l^{mdwf}	am_s^{mdwf}
a15m310	1.3	12	1.50	0.50	1.0	0.01580	0.0902
a12m310	1.2	8	1.25	0.25	1.0	0.01260	0.0693
a09m310	1.1	6	1.25	0.25	1.0	0.00951	0.0491
a15m220	1.3	16	1.75	0.75	1.0	0.00712	0.0902
a12m220	1.2	12	1.50	0.50	1.0	0.00600	0.0693
a09m220	1.1	8	1.25	0.25	1.0	0.00449	0.0491
a15m130	1.3	24	2.25	1.25	1.0	0.00216	0.0902
a12m135	1.2	20	2.00	1.00	1.0	0.00195	0.0693

TABLE IV. Tuned MDWF parameters for our MALQCD calculations, used for example in Ref. [137].

C. Tuned parameters

Finally, we report the tuned values of the MDWF parameters used in these MALQCD calculations. The MDWF quark masses were chosen such that the MDWF pseudoscalar masses (m_π and m_{ss}) would match the corresponding HISQ taste-5 pseudoscalar masses to within 2%. In Table IV, we list the resulting MDWF parameters. These parameters were used in Ref. [137].

IV. MDWF IN QUDA: OPTIMIZATIONS AND PERFORMANCE

In order to efficiently perform the MDWF solves, we utilize the GPU implementation of the MDWF operator and solver [146] from the highly optimized QUDA library [147, 148]. We added the API for accessing this solver to the Chroma [108] package, which is publicly available in the most recent version.

The MDWF calculations were performed on three different GPU enabled machines, Surface and RZHasGPU at LLNL and Titan at OLCF.¹ The Surface cluster is composed of dual NVIDIA Tesla K40 cards with Intel

¹ Some of the early tuning and flow time dependence studies were performed at the JLab High Performance Computing Center and at the Fermilab Lattice Gauge Theory Computational Facility.

computer	GPUs	MPI ranks	geometry	performance [GFlops]		
				total	per node	% peak
Surface	2	2	1 1 1 2	1250	1250	44%
RZHasGPU	4	4	1 1 1 4	1785	1785	48%
Titan	8	16	1 1 2 8	2885	361	25%
Titan	16	32	1 2 2 8	4720	295	20%
Titan	32	64	1 2 4 8	8500	266	18%

TABLE V. Performance of the double-half mixed precision MDWF solver in QUDA on the various compute nodes used with 2, 4 and 1 GPU per node on the Surface, RZHasGPU and Titan computers. The % of peak performance is obtained by comparing our sustained to the theoretical single-node single-precision performance. On Titan, we oversubscribe the GPUs by using 1 MPI rank per NUMA node, which amounts to 2 MPI ranks per GPU, resulting in a $\sim 69\%$ performance boost.

Xeon E5-2670 CPU nodes. The RZHasGPU cluster is composed of dual NVIDIA Tesla K80 cards with Intel Xeon E5-2667 v3 CPU nodes. The Titan supercomputer is composed of single NVIDIA Tesla K20X cards with AMD Opteron CPU nodes. An interesting feature of the Titan nodes is the use of two 8-core NUMA nodes per node. We have found that we can provide 2 MPI ranks per GPU, by using both NUMA nodes, and achieve approximately 69% performance boost with otherwise identical parameters. In Table V we list the sustained performance on the three machines achieved with the present implementation of the double-half mixed-precision MDWF solver. The single node performance is notable and we are at present working on improving the strong scaling of the MDWF solver in QUDA through better overlapping of communication and computation. Additionally, a significant reduction of the condition number for the symmetric implementation of the MDWF operator has been observed [149]. QUDA supports both the symmetric and asymmetric implementations of the MDWF operator. Currently, Chroma only supports the asymmetric operator, but we plan to investigate possible reduction in time-to-solution from switching to the symmetric implementation.

V. CONCLUSIONS

In this work, we have motivated a new mixed lattice QCD action: Möbius Domain-Wall valence fermions solved with the dynamical $N_f = 2 + 1 + 1$ HISQ sea fermions after a gradient smearing algorithm is used to filter out UV modes of the gluons. To retain the correct continuum limit, the gradient flow time is held fixed in lattice units, such that any dependence upon this new scale also vanishes in the continuum limit. We demonstrate the flow time independence of the continuum limit by computing two sample quantities, F_K/F_π and m_N/F_π . Of particular note, we also demonstrate

that the gradient flow smearing highly suppresses sources of residual chiral symmetry breaking in the action for moderate values of the flow time: the axial renormalization constant becomes effectively lattice spacing independent and close to 1 for all ensembles at a flow time of $t_{gf} = 1$; the residual chiral symmetry breaking, measured by the quantity m_{res} , is exponentially damped with increasing flow time, and less than 10% of the input light quark mass for all ensembles, including the physical quark mass ensembles, with $t_{gf} = 1$ and moderate values of L_5 .

This action, coupled with the use of the highly optimized QUDA library, provides an economical method of performing LQCD calculations with an action that respects chiral symmetry to a high degree. The MILC Collaboration has a long history of making their configurations freely available to all interested parties. The breadth of parameters used in the generation of the HISQ ensembles allows users to fully control all LQCD systematics: notably the continuum, and infinite volume extrapolations, as well as a physical quark mass interpolation.

We have plans to use this action for computing various quantities relevant to fundamental nuclear and high-energy physics research, detailed for example in the NSAC Long Range Plan for Nuclear Science and the HEPAP P5 Strategic Plan for U.S. Particle Physics. So far, we have used this mixed action to demonstrate the benefits of a new method for computing hadronic matrix elements [138] and we have computed the $\pi^- \rightarrow \pi^+$ transition matrix elements relevant for scenario that heavy lepton-number violating physics beyond the Standard Model contributes to the hypothesized neutrinoless double beta decay of large nuclei [137].

ACKNOWLEDGMENTS

We gratefully acknowledge the MILC Collaboration for use of the dynamical HISQ ensembles [107]. We thank Carleton DeTar and Doug Toussaint for help compiling and using the MILC code at LLNL and understanding how to write source fields from Chroma that can be read by MILC for the construction of the mixed-meson correlation functions. We also thank Claude Bernard for useful correspondence regarding scale setting and taste violations with the HISQ action. Part of this work was performed at the Kavli Institute for Theoretical Physics supported by NSF Grant No. PHY-1125915.

The software used for this work was built on top of the Chroma software suite [108] and the highly optimized QCD GPU library QUDA [147, 148]. We also utilized the highly efficient HDF5 I/O Library [150] with an interface to HDF5 in the USQCD Software Stack added with SciDAC 3 support (CallLat) [151], as well as the MILC software for solving for HISQ propagators. Finally, the HPC jobs were efficiently managed with a bash job manager, METAQ [152], capable of intelligently backfilling idle

nodes in sets of nodes bundled into larger jobs submitted to HPC systems. METAQ was developed with SciDAC 3 support (CalLat) and is available on [github](#). The numerical calculations in this work were performed at: the Jefferson Lab High Performance Computing Center and the Fermilab Lattice Gauge Theory Computational Facility on facilities of the USQCD Collaboration, which are funded by the Office of Science of the U.S. Department of Energy; Lawrence Livermore National Laboratory on the Surface and RZhasGPU GPU clusters as well as the Cab CPU and Vulcan BG/Q clusters; and the Oak Ridge Leadership Computing Facility at the Oak Ridge National Laboratory, which is supported by the Office of Science of the U.S. Department of Energy under Contract No. DE-AC05-00OR22725, on the Titan machine through a DOE INCITE award (CalLat). We thank the Lawrence Livermore National Laboratory (LLNL) Institutional Computing Grand Challenge program for the computing allocation.

This work was performed with support from LDRD funding from LLNL 13-ERD-023 (EB, ER, PV); and by the RIKEN Special Postdoctoral Researcher program (ER). This work was also performed under the auspices of the U.S. Department of Energy by Lawrence Liver-

more National Laboratory under Contract DE-AC52-07NA27344 (EB, ER, PV); under contract DE-AC05-06OR23177, under which Jefferson Science Associates, LLC, manages and operates the Jefferson Lab (BJ, KO); under contract DE-AC02-05CH11231, which the Regents of the University of California manage and operate Lawrence Berkeley National Laboratory and the National Energy Research Scientific Computing Center (CCC, TK, AWL); This work was further performed under the auspices of the U.S. Department of Energy, Office of Science, Office of Nuclear Physics under contracts: DE-FG02-04ER41302 (CMB, KNO); DE-SC00046548 (AN); DE-SC0015376, Double-Beta Decay Topical Collaboration (AWL); by the Office of Advanced Scientific Computing Research, Scientific Discovery through Advanced Computing (SciDAC) program under Award Number KB0301052 (EB, TK, AWL); and by the DOE Early Career Research Program, Office of Nuclear Physics under FWP NQCDAWL (CCC, AWL).

Appendix A: Tables of flow time dependence

Here, we provide tables of the various quantities computed in this work on the different flow times used.

-
- [1] H. Fritzsch and M. Gell-Mann, *Proceedings, 16th International Conference on High-Energy Physics, ICHEP, Batavia, Illinois, 6-13 Sep 1972, eConf C720906V2*, 135 (1972), [arXiv:hep-ph/0208010 \[hep-ph\]](#).
 - [2] H. Fritzsch, M. Gell-Mann, and H. Leutwyler, *Phys. Lett.* **B47**, 365 (1973).
 - [3] D. J. Gross and F. Wilczek, *Phys. Rev. Lett.* **30**, 1343 (1973).
 - [4] H. D. Politzer, *Phys. Rev. Lett.* **30**, 1346 (1973).
 - [5] S. Weinberg, *Physica* **A96**, 327 (1979).
 - [6] K. Symanzik, *Nucl. Phys.* **B226**, 187 (1983).
 - [7] K. Symanzik, *Nucl. Phys.* **B226**, 205 (1983).
 - [8] S. Aoki *et al.*, (2016), [arXiv:1607.00299 \[hep-lat\]](#).
 - [9] K. G. Wilson, *Phys. Rev.* **D10**, 2445 (1974).
 - [10] B. Sheikholeslami and R. Wohlert, *Nucl. Phys.* **B259**, 572 (1985).
 - [11] R. Frezzotti, P. A. Grassi, S. Sint, and P. Weiss (Alpha), *JHEP* **08**, 058 (2001), [arXiv:hep-lat/0101001 \[hep-lat\]](#).
 - [12] R. Frezzotti and G. C. Rossi, *JHEP* **08**, 007 (2004), [arXiv:hep-lat/0306014 \[hep-lat\]](#).
 - [13] J. B. Kogut and L. Susskind, *Phys. Rev.* **D11**, 395 (1975).
 - [14] L. Susskind, *Phys. Rev.* **D16**, 3031 (1977).
 - [15] E. Marinari, G. Parisi, and C. Rebbi, *Nucl. Phys.* **B190**, 734 (1981), [595(1981)].
 - [16] C. Bernard, M. Golterman, Y. Shamir, and S. R. Sharpe, *Phys. Lett.* **B649**, 235 (2007), [arXiv:hep-lat/0603027 \[hep-lat\]](#).
 - [17] C. Bernard, M. Golterman, and Y. Shamir, *Phys. Rev.* **D73**, 114511 (2006), [arXiv:hep-lat/0604017 \[hep-lat\]](#).
 - [18] M. Creutz, *Phys. Lett.* **B649**, 230 (2007), [arXiv:hep-lat/0701018 \[hep-lat\]](#).
 - [19] C. Bernard, *Phys. Rev.* **D71**, 094020 (2005), [arXiv:hep-lat/0412030 \[hep-lat\]](#).
 - [20] C. Bernard, *Phys. Rev.* **D73**, 114503 (2006), [arXiv:hep-lat/0603011 \[hep-lat\]](#).
 - [21] Y. Shamir, *Phys. Rev.* **D71**, 034509 (2005), [arXiv:hep-lat/0412014 \[hep-lat\]](#).
 - [22] Y. Shamir, *Phys. Rev.* **D75**, 054503 (2007), [arXiv:hep-lat/0607007 \[hep-lat\]](#).
 - [23] C. Bernard, M. Golterman, and Y. Shamir, *Phys. Rev.* **D77**, 074505 (2008), [arXiv:0712.2560 \[hep-lat\]](#).
 - [24] S. Durr and C. Hoelbling, *Phys. Rev.* **D71**, 054501 (2005), [arXiv:hep-lat/0411022 \[hep-lat\]](#).
 - [25] S. Durr and C. Hoelbling, *Phys. Rev.* **D74**, 014513 (2006), [arXiv:hep-lat/0604005 \[hep-lat\]](#).
 - [26] A. Hasenfratz and R. Hoffmann, *Phys. Rev.* **D74**, 014511 (2006), [arXiv:hep-lat/0604010 \[hep-lat\]](#).
 - [27] C. Bernard, M. Golterman, Y. Shamir, and S. R. Sharpe, *Phys. Rev.* **D77**, 114504 (2008), [arXiv:0711.0696 \[hep-lat\]](#).
 - [28] S. R. Sharpe, *Proceedings, 24th International Symposium on Lattice Field Theory (Lattice 2006): Tucson, USA, July 23-28, 2006, PoS LAT2006*, 022 (2006), [arXiv:hep-lat/0610094 \[hep-lat\]](#).
 - [29] A. S. Kronfeld, *Proceedings, 25th International Symposium on Lattice field theory (Lattice 2007): Regensburg, Germany, July 30-August 4, 2007, PoS LAT2007*, 016 (2007), [arXiv:0711.0699 \[hep-lat\]](#).
 - [30] A. Bazavov *et al.* (MILC), *Rev. Mod. Phys.* **82**, 1349 (2010), [arXiv:0903.3598 \[hep-lat\]](#).

ensemble	M_5	L_5	b_5	c_5	t_{gf}	plaq.	am_l^{mdwf}	am_l^{res}	am_π	am_s^{mdwf}	am_s^{res}	am_{ss}
a15m310	1.3	12	1.5	0.5	0.2	0.87701(2)	0.00970	0.003904(42)	0.2354(09)	0.06810	0.003023(29)	0.5158(07)
					0.4	0.95521(1)	0.01160	0.002339(29)	0.2314(10)	0.07380	0.001687(21)	0.5153(06)
					0.6	0.97723(1)	0.01250	0.001693(27)	0.2256(09)	0.08000	0.001179(19)	0.5156(08)
					0.8	0.98560(1)	0.01480	0.001302(26)	0.2339(08)	0.08520	0.000877(16)	0.5165(07)
					1.0	0.98964(1)	0.01580	0.001012(22)	0.2339(08)	0.09020	0.000671(15)	0.5182(07)
a12m310	1.2	8	1.25	0.25	0.2	0.89320(1)	0.00680	0.004286(29)	0.1888(07)	0.05300	0.003382(23)	0.4188(06)
					0.4	0.96401(1)	0.00960	0.001945(23)	0.1890(06)	0.05830	0.001344(17)	0.4182(06)
					0.6	0.98251(1)	0.01086	0.001357(23)	0.1889(06)	0.06280	0.000873(15)	0.4186(06)
					0.8	0.98925(0)	0.01176	0.001040(21)	0.1885(06)	0.06650	0.000632(13)	0.4192(06)
					1.0	0.99242(0)	0.01260	0.000825(17)	0.1889(05)	0.06930	0.000482(11)	0.4188(06)
a09m310	1.1	6	1.25	0.25	0.2	0.91073(0)	0.00543	0.002722(13)	0.1400(04)	0.03880	0.002377(11)	0.3121(03)
					0.4	0.97236(0)	0.00798	0.000625(09)	0.1415(04)	0.04330	0.000462(07)	0.3139(03)
					0.6	0.98721(0)	0.00850	0.000375(08)	0.1398(04)	0.04500	0.000258(05)	0.3104(03)
					0.8	0.99239(0)	0.00921	0.000289(08)	0.1413(04)	0.04780	0.000201(04)	0.3128(04)
					1.0	0.99478(0)	0.00951	0.000243(07)	0.1409(04)	0.04910	0.000178(04)	0.3113(04)
a15m220	1.3	16	1.75	0.75	0.2	0.87718(1)	0.00425	0.002265(17)	0.1700(07)	0.06810	0.001727(16)	0.5118(06)
					0.4	0.95535(1)	0.00532	0.001349(15)	0.1672(09)	0.07380	0.000959(12)	0.5125(06)
					0.6	0.97735(1)	0.00615	0.000966(17)	0.1673(08)	0.08000	0.000662(11)	0.5120(06)
					0.8	0.98570(1)	0.00668	0.000731(16)	0.1653(14)	0.08520	0.000491(10)	0.5119(06)
					1.0	0.98973(1)	0.00712	0.000577(11)	0.1644(10)	0.09020	0.000365(10)	0.5140(05)
a12m220	1.2	12	1.5	0.5	0.2	0.89332(1)	0.00365	0.001558(12)	0.1330(06)	0.05480	0.001087(11)	0.4169(04)
					0.4	0.96410(0)	0.00456	0.000933(10)	0.1341(06)	0.05880	0.000590(08)	0.4174(04)
					0.6	0.98259(0)	0.00522	0.000667(09)	0.1348(05)	0.06280	0.000397(07)	0.4167(05)
					0.8	0.98931(0)	0.00575	0.000509(07)	0.1357(05)	0.06660	0.000280(06)	0.4172(04)
					1.0	0.99248(0)	0.00600	0.000397(06)	0.1346(05)	0.06930	0.000216(04)	0.4168(05)

TABLE VI. The tuned values of the MDWF quark masses on various ensembles for various flow times. We also list the values of the average plaquette after applying the gradient flow as well as the fitted pion and $\bar{s}\gamma_5 s$ masses using a single-cosh fit in the middle time region.

- [31] H. B. Nielsen and M. Ninomiya, *Nucl. Phys.* **B185**, 20 (**1981**), [,533(1980)].
- [32] H. B. Nielsen and M. Ninomiya, *Nucl. Phys.* **B193**, 173 (**1981**).
- [33] H. B. Nielsen and M. Ninomiya, *Phys. Lett.* **B105**, 219 (**1981**).
- [34] P. H. Ginsparg and K. G. Wilson, *Phys. Rev.* **D25**, 2649 (**1982**).
- [35] M. Lüscher, *Phys. Lett.* **B428**, 342 (1998), arXiv:hep-lat/9802011 [hep-lat].
- [36] D. B. Kaplan, *Phys. Lett.* **B288**, 342 (1992), arXiv:hep-lat/9206013 [hep-lat].
- [37] Y. Shamir, *Nucl. Phys.* **B406**, 90 (1993), arXiv:hep-lat/9303005 [hep-lat].
- [38] V. Furman and Y. Shamir, *Nucl. Phys.* **B439**, 54 (1995), arXiv:hep-lat/9405004 [hep-lat].
- [39] R. Narayanan and H. Neuberger, *Nucl. Phys.* **B412**, 574 (1994), arXiv:hep-lat/9307006 [hep-lat].
- [40] R. Narayanan and H. Neuberger, *Phys. Rev. Lett.* **71**, 3251 (1993), arXiv:hep-lat/9308011 [hep-lat].
- [41] R. Narayanan and H. Neuberger, *Nucl. Phys.* **B443**, 305 (1995), arXiv:hep-th/9411108 [hep-th].
- [42] A. Borici, *Lattice field theory. Proceedings, 17th International Symposium, Lattice'99, Pisa, Italy, June 29 July 3, 1999*, *Nucl. Phys. Proc. Suppl.* **83**, 771 (2000), arXiv:hep-lat/9909057 [hep-lat].
- [43] A. Borici, in *Lattice fermions and structure of the vacuum. Proceedings, NATO Advanced Research Workshop, Dubna, Russia, October 5-9, 1999* (1999) pp. 41–52, arXiv:hep-lat/9912040 [hep-lat].
- [44] A. D. Kennedy, *Lattice field theory. Proceedings, 22nd International Symposium, Lattice 2004, Batavia, USA, June 21-26, 2004*, *Nucl. Phys. Proc. Suppl.* **140**, 190 (2005), [,190(2004)], arXiv:hep-lat/0409167 [hep-lat].
- [45] O. Bar, G. Rupak, and N. Shores, *Phys. Rev.* **D67**, 114505 (2003), arXiv:hep-lat/0210050 [hep-lat].
- [46] D. B. Renner, W. Schroers, R. Edwards, G. T. Fleming, P. Hagler, J. W. Negele, K. Orginos, A. V. Pochinski, and D. Richards (LHP), *Lattice field theory. Proceedings, 22nd International Symposium, Lattice 2004, Batavia, USA, June 21-26, 2004*, *Nucl. Phys. Proc. Suppl.* **140**, 255 (2005), [,255(2004)], arXiv:hep-lat/0409130 [hep-lat].
- [47] K. Orginos and D. Toussaint (MILC), *Phys. Rev.* **D59**, 014501 (1999), arXiv:hep-lat/9805009 [hep-lat].
- [48] K. Orginos, D. Toussaint, and R. L. Sugar (MILC), *Phys. Rev.* **D60**, 054503 (1999), arXiv:hep-lat/9903032 [hep-lat].

ensemble	t_{gf}	Z_A^{ll}	Z_A^{ls}	aF_π	aF_K	am_N	F_K/F_π	m_N/F_π
a15m310	0.2	0.8701(22)	0.87484(76)	0.07690(75)	0.08639(79)	0.841(32)	1.1234(61)	10.94(43)
	0.4	0.9021(22)	0.90742(71)	0.07652(64)	0.08493(63)	0.832(20)	1.1099(64)	10.87(28)
	0.6	0.9312(23)	0.93891(68)	0.07552(58)	0.08377(51)	0.822(16)	1.1093(66)	10.89(23)
	0.8	0.9520(22)	0.96116(71)	0.07478(56)	0.08316(40)	0.825(12)	1.1122(66)	11.03(19)
	1.0	0.9657(21)	0.97657(72)	0.07382(55)	0.08231(39)	0.820(11)	1.1150(65)	11.11(17)
a12m310	0.2	0.9001(26)	0.90369(92)	0.06348(68)	0.07117(64)	0.682(23)	1.1213(52)	10.74(38)
	0.4	0.9190(23)	0.92416(79)	0.06276(56)	0.06986(48)	0.667(23)	1.1132(45)	10.62(37)
	0.6	0.9406(20)	0.94600(68)	0.06222(49)	0.06895(40)	0.659(22)	1.1081(42)	10.60(36)
	0.8	0.9541(18)	0.96026(59)	0.06164(44)	0.06819(36)	0.657(20)	1.1062(41)	10.66(33)
	1.0	0.9631(17)	0.96988(52)	0.06109(41)	0.06755(33)	0.656(19)	1.1057(39)	10.74(31)
a09m310	0.2	0.9326(21)	0.93479(63)	0.04565(44)	0.05152(45)	0.486(20)	1.1285(50)	10.64(45)
	0.4	0.9416(16)	0.94469(48)	0.04580(34)	0.05140(34)	0.488(18)	1.1223(41)	10.66(41)
	0.6	0.9551(14)	0.95854(43)	0.04556(31)	0.05099(30)	0.490(16)	1.1191(38)	10.76(36)
	0.8	0.9640(13)	0.96742(37)	0.04531(29)	0.05081(28)	0.488(13)	1.1214(35)	10.78(31)
	1.0	0.9693(12)	0.97330(34)	0.04510(28)	0.05046(26)	0.472(15)	1.1188(36)	10.47(35)
a15m220	0.2	0.8646(22)	0.87148(51)	0.07556(75)	0.08768(67)	0.761(29)	1.1603(69)	10.08(40)
	0.4	0.8925(18)	0.90568(46)	0.07461(63)	0.08596(54)	0.796(13)	1.1521(72)	10.67(19)
	0.6	0.9224(15)	0.93803(38)	0.07338(56)	0.08416(48)	0.789(11)	1.1470(68)	10.76(17)
	0.8	0.9432(14)	0.95979(40)	0.07240(53)	0.08275(43)	0.775(12)	1.1428(65)	10.71(18)
	1.0	0.9587(14)	0.97529(33)	0.07103(51)	0.08150(40)	0.762(12)	1.1473(63)	10.73(19)
a12m220	0.2	0.8909(34)	0.90103(83)	0.05720(67)	0.06673(59)	0.636(25)	1.1666(82)	11.13(45)
	0.4	0.9103(26)	0.92212(61)	0.05753(55)	0.06657(46)	0.631(29)	1.1571(72)	10.97(51)
	0.6	0.9339(22)	0.94500(48)	0.05748(49)	0.06598(40)	0.622(27)	1.1480(65)	10.83(47)
	0.8	0.9508(19)	0.96015(41)	0.05746(44)	0.06541(35)	0.616(25)	1.1385(59)	10.73(44)
	1.0	0.9589(17)	0.97003(37)	0.05700(42)	0.06481(32)	0.611(25)	1.1370(60)	10.72(44)

TABLE VII. Various hadronic quantities and renormalization constants determined at different flow times. The posterior distributions related to meson correlation functions are extracted using a $2+2$ state fit ansatz (normal and oscillating states), the proton correlator uses a 2 state fit ansatz, while m_{res} is extracted from a constant fit. The meson two-point correlation functions are fit simultaneously with the 4D axial-vector current, and then a chained fit [153] is used to propagate all remaining correlations. The entire fit strategy is implemented under the Bayesian framework with `1sqfit` [154].

- [49] C. W. Bernard, T. Burch, K. Orginos, D. Toussaint, T. A. DeGrand, C. E. Detar, S. Datta, S. A. Gottlieb, U. M. Heller, and R. Sugar, *Phys. Rev.* **D64**, 054506 (2001), arXiv:hep-lat/0104002 [hep-lat].
- [50] R. G. Edwards, G. T. Fleming, P. Hagler, J. W. Negele, K. Orginos, A. V. Pochinsky, D. B. Renner, D. G. Richards, and W. Schroers (LHPC), *Phys. Rev. Lett.* **96**, 052001 (2006), arXiv:hep-lat/0510062 [hep-lat].
- [51] P. Hagler *et al.* (LHPC), *Phys. Rev.* **D77**, 094502 (2008), arXiv:0705.4295 [hep-lat].
- [52] J. D. Bratt *et al.* (LHPC), *Phys. Rev.* **D82**, 094502 (2010), arXiv:1001.3620 [hep-lat].
- [53] S. R. Beane, P. F. Bedaque, K. Orginos, and M. J. Savage (NPLQCD), *Phys. Rev. Lett.* **97**, 012001 (2006), arXiv:hep-lat/0602010.
- [54] S. R. Beane *et al.* (NPLQCD), *Phys. Rev.* **D77**, 014505 (2008), arXiv:0706.3026 [hep-lat].
- [55] A. Walker-Loud *et al.*, *Phys. Rev.* **D79**, 054502 (2009), arXiv:0806.4549 [hep-lat].
- [56] C. Aubin, J. Laiho, and R. S. Van de Water, *Phys. Rev.* **D81**, 014507 (2010), arXiv:0905.3947 [hep-lat].
- [57] P. Langacker and H. Pagels, *Phys. Rev.* **D8**, 4595 (1973).
- [58] J. Gasser and H. Leutwyler, *Annals Phys.* **158**, 142 (1984).
- [59] H. Leutwyler, *Annals Phys.* **235**, 165 (1994), arXiv:hep-ph/9311274 [hep-ph].
- [60] S. R. Sharpe and R. L. Singleton, Jr, *Phys. Rev.* **D58**, 074501 (1998), arXiv:hep-lat/9804028 [hep-lat].
- [61] O. Bar, G. Rupak, and N. Shores, *Phys. Rev.* **D70**, 034508 (2004), arXiv:hep-lat/0306021 [hep-lat].
- [62] O. Bar, C. Bernard, G. Rupak, and N. Shores, *Phys. Rev.* **D72**, 054502 (2005), arXiv:hep-lat/0503009 [hep-lat].
- [63] B. C. Tiburzi, *Phys. Rev.* **D72**, 094501 (2005), [Erratum: *Phys. Rev.* D79, 039904(2009)], arXiv:hep-lat/0508019 [hep-lat].
- [64] J.-W. Chen, D. O'Connell, R. S. Van de Water, and A. Walker-Loud, *Phys. Rev.* **D73**, 074510 (2006), arXiv:hep-lat/0510024 [hep-lat].
- [65] J.-W. Chen, D. O'Connell, and A. Walker-Loud, *Phys. Rev.* **D75**, 054501 (2007), arXiv:hep-lat/0611003 [hep-lat].

- [66] K. Orginos and A. Walker-Loud, *Phys. Rev.* **D77**, 094505 (2008), arXiv:0705.0572 [hep-lat].
- [67] F.-J. Jiang, (2007), arXiv:hep-lat/0703012 [hep-lat].
- [68] J.-W. Chen, D. O'Connell, and A. Walker-Loud, *JHEP* **04**, 090 (2009), arXiv:0706.0035 [hep-lat].
- [69] J.-W. Chen, M. Golterman, D. O'Connell, and A. Walker-Loud, *Phys. Rev.* **D79**, 117502 (2009), arXiv:0905.2566 [hep-lat].
- [70] C. W. Bernard and M. F. L. Golterman, *Phys. Rev.* **D49**, 486 (1994), arXiv:hep-lat/9306005 [hep-lat].
- [71] S. R. Sharpe and N. Shores, *Phys. Rev.* **D62**, 094503 (2000), arXiv:hep-lat/0006017 [hep-lat].
- [72] S. R. Sharpe and N. Shores, *Phys. Rev.* **D64**, 114510 (2001), arXiv:hep-lat/0108003 [hep-lat].
- [73] J.-W. Chen and M. J. Savage, *Phys. Rev.* **D65**, 094001 (2002), arXiv:hep-lat/0111050 [hep-lat].
- [74] S. R. Sharpe and R. S. Van de Water, *Phys. Rev.* **D69**, 054027 (2004), arXiv:hep-lat/0310012 [hep-lat].
- [75] D. Arndt and B. C. Tiburzi, *Phys. Rev.* **D68**, 094501 (2003), arXiv:hep-lat/0307003 [hep-lat].
- [76] A. Walker-Loud, *Nucl. Phys.* **A747**, 476 (2005), arXiv:hep-lat/0405007 [hep-lat].
- [77] C. Bernard and M. Golterman, *Proceedings, 28th International Symposium on Lattice field theory (Lattice 2010): Villasimius, Italy, June 14-19, 2010*, PoS **LATTICE2010**, 252 (2010), arXiv:1011.0184 [hep-lat].
- [78] C. Bernard and M. Golterman, *Phys. Rev.* **D88**, 014004 (2013), arXiv:1304.1948 [hep-lat].
- [79] S. R. Beane and M. J. Savage, *Nucl. Phys.* **A709**, 319 (2002), arXiv:hep-lat/0203003 [hep-lat].
- [80] S. R. Beane and M. J. Savage, *Phys. Rev.* **D67**, 054502 (2003), arXiv:hep-lat/0210046 [hep-lat].
- [81] D. Arndt and B. C. Tiburzi, *Phys. Rev.* **D68**, 114503 (2003), [Erratum: *Phys. Rev.* D69, 059904(2004)], arXiv:hep-lat/0308001 [hep-lat].
- [82] D. Arndt and B. C. Tiburzi, *Phys. Rev.* **D69**, 014501 (2004), arXiv:hep-lat/0309013 [hep-lat].
- [83] B. C. Tiburzi and A. Walker-Loud, *Nucl. Phys.* **A748**, 513 (2005), arXiv:hep-lat/0407030 [hep-lat].
- [84] B. C. Tiburzi, *Phys. Rev.* **D71**, 034501 (2005), arXiv:hep-lat/0410033 [hep-lat].
- [85] B. C. Tiburzi and A. Walker-Loud, *Nucl. Phys.* **A764**, 274 (2006), arXiv:hep-lat/0501018 [hep-lat].
- [86] D. O'Connell and M. J. Savage, *Phys. Lett.* **B633**, 319 (2006), arXiv:hep-lat/0508009 [hep-lat].
- [87] S. Prelovsek, *Phys. Rev.* **D73**, 014506 (2006), arXiv:hep-lat/0510080 [hep-lat].
- [88] C. Aubin, J. Laiho, and R. S. Van de Water, *Phys. Rev.* **D77**, 114501 (2008), arXiv:0803.0129 [hep-lat].
- [89] H. Na, C. M. Bouchard, G. P. Lepage, C. Monahan, and J. Shigemitsu (HPQCD), *Phys. Rev.* **D92**, 054510 (2015), [Erratum: *Phys. Rev.* D93,no.11,119906(2016)], arXiv:1505.03925 [hep-lat].
- [90] G. C. Donald, C. T. H. Davies, J. Koponen, and G. P. Lepage, *Phys. Rev. Lett.* **112**, 212002 (2014), arXiv:1312.5264 [hep-lat].
- [91] A. Li *et al.* (xQCD), *Phys. Rev.* **D82**, 114501 (2010), arXiv:1005.5424 [hep-lat].
- [92] M. Lujan, A. Alexandru, Y. Chen, T. Draper, W. Freeman, M. Gong, F. X. Lee, A. Li, K. F. Liu, and N. Mathur, *Phys. Rev.* **D86**, 014501 (2012), arXiv:1204.6256 [hep-lat].
- [93] M. Gong *et al.* (XQCD), *Phys. Rev.* **D88**, 014503 (2013), arXiv:1304.1194 [hep-ph].
- [94] C. Allton *et al.* (RBC, UKQCD), *Phys. Rev.* **D76**, 014504 (2007), arXiv:hep-lat/0701013 [hep-lat].
- [95] Y. Aoki *et al.* (RBC, UKQCD), *Phys. Rev.* **D83**, 074508 (2011), arXiv:1011.0892 [hep-lat].
- [96] T. Bhattacharya, S. D. Cohen, R. Gupta, A. Joseph, H.-W. Lin, and B. Yoon, *Phys. Rev.* **D89**, 094502 (2014), arXiv:1306.5435 [hep-lat].
- [97] T. Bhattacharya, V. Cirigliano, S. Cohen, R. Gupta, A. Joseph, H.-W. Lin, and B. Yoon (PNDME), *Phys. Rev.* **D92**, 094511 (2015), arXiv:1506.06411 [hep-lat].
- [98] S. Durr *et al.*, *Phys. Rev.* **D85**, 014509 (2012), [Erratum: *Phys. Rev.* D93,no.3,039905(2016)], arXiv:1109.4265 [hep-lat].
- [99] S. Durr *et al.*, *Phys. Rev. Lett.* **116**, 172001 (2016), arXiv:1510.08013 [hep-lat].
- [100] Y.-B. Yang, A. Alexandru, T. Draper, J. Liang, and K.-F. Liu (xQCD), *Phys. Rev.* **D94**, 054503 (2016), arXiv:1511.09089 [hep-lat].
- [101] R. S. Sufian, Y.-B. Yang, A. Alexandru, T. Draper, K.-F. Liu, and J. Liang, (2016), arXiv:1606.07075 [hep-ph].
- [102] T. Bhattacharya, V. Cirigliano, S. Cohen, R. Gupta, H.-W. Lin, and B. Yoon, *Phys. Rev.* **D94**, 054508 (2016), arXiv:1606.07049 [hep-lat].
- [103] S. Borsanyi *et al.* (Budapest-Marseille-Wuppertal), *Phys. Rev. Lett.* **111**, 252001 (2013), arXiv:1306.2287 [hep-lat].
- [104] S. Borsanyi *et al.*, *Science* **347**, 1452 (2015), arXiv:1406.4088 [hep-lat].
- [105] D. A. Brantley, B. Joo, E. V. Mastropas, E. Mereghetti, H. Monge-Camacho, B. C. Tiburzi, and A. Walker-Loud, (2016), arXiv:1612.07733 [hep-lat].
- [106] E. Follana, Q. Mason, C. Davies, K. Hornbostel, G. P. Lepage, J. Shigemitsu, H. Trottier, and K. Wong (HPQCD, UKQCD), *Phys. Rev.* **D75**, 054502 (2007), arXiv:hep-lat/0610092 [hep-lat].
- [107] A. Bazavov *et al.* (MILC), *Phys. Rev.* **D87**, 054505 (2013), arXiv:1212.4768 [hep-lat].
- [108] R. G. Edwards and B. Joo (SciDAC Collaboration, LHPC Collaboration, UKQCD Collaboration), *Nucl.Phys.Proc.Supp.* **140**, 832 (2005), arXiv:hep-lat/0409003 [hep-lat].
- [109] S. R. Beane, K. Orginos, and M. J. Savage (NPLQCD), *Int. J. Mod. Phys.* **E17**, 1157 (2008), arXiv:0805.4629 [hep-lat].
- [110] R. C. Brower, H. Neff, and K. Orginos, *Lattice field theory. Proceedings, 22nd International Symposium, Lattice 2004, Batavia, USA, June 21-26, 2004*, *Nucl. Phys. Proc. Suppl.* **140**, 686 (2005), [,686(2004)], arXiv:hep-lat/0409118 [hep-lat].
- [111] R. C. Brower, H. Neff, and K. Orginos, *Hadron physics, proceedings of the Workshop on Computational Hadron Physics, University of Cyprus, Nicosia, Cyprus, 14-17 September 2005*, *Nucl. Phys. Proc. Suppl.* **153**, 191 (2006), arXiv:hep-lat/0511031 [hep-lat].
- [112] R. C. Brower, H. Neff, and K. Orginos, (2012), arXiv:1206.5214 [hep-lat].
- [113] H. Neuberger, *Phys. Rev.* **D57**, 5417 (1998), arXiv:hep-lat/9710089 [hep-lat].
- [114] H. Neuberger, *Phys. Lett.* **B417**, 141 (1998), arXiv:hep-lat/9707022 [hep-lat].
- [115] P. M. Vranas, *Phys. Rev.* **D57**, 1415 (1998), arXiv:hep-lat/9705023 [hep-lat].

- [116] Y. Kikukawa and T. Noguchi, *Lattice field theory. Proceedings, 17th International Symposium, Lattice'99, Pisa, Italy, June 29-July 3, 1999*, Nucl. Phys. Proc. Suppl. **83**, 630 (2000), arXiv:hep-lat/9902022 [hep-lat].
- [117] R. G. Edwards and U. M. Heller, Phys. Rev. **D63**, 094505 (2001), arXiv:hep-lat/0005002 [hep-lat].
- [118] A. D. Kennedy, (2006), arXiv:hep-lat/0607038 [hep-lat].
- [119] A. Hasenfratz and F. Knechtli, Phys. Rev. **D64**, 034504 (2001), arXiv:hep-lat/0103029 [hep-lat].
- [120] T. A. DeGrand, A. Hasenfratz, and T. G. Kovacs, Phys. Rev. **D67**, 054501 (2003), arXiv:hep-lat/0211006 [hep-lat].
- [121] T. A. DeGrand (MILC), Phys. Rev. **D69**, 014504 (2004), arXiv:hep-lat/0309026 [hep-lat].
- [122] S. Durr, C. Hoelbling, and U. Wenger, Phys. Rev. **D70**, 094502 (2004), arXiv:hep-lat/0406027 [hep-lat].
- [123] R. Narayanan and H. Neuberger, JHEP **0603**, 064 (2006), arXiv:hep-th/0601210 [hep-th].
- [124] M. Lüscher and P. Weisz, JHEP **1102**, 051 (2011), arXiv:1101.0963 [hep-th].
- [125] M. Lüscher, JHEP **1304**, 123 (2013), arXiv:1302.5246 [hep-lat].
- [126] C. Morningstar and M. J. Peardon, Phys. Rev. **D69**, 054501 (2004), arXiv:hep-lat/0311018 [hep-lat].
- [127] L. Del Debbio, A. Patella, and A. Rago, JHEP **1311**, 212 (2013), arXiv:1306.1173 [hep-th].
- [128] H. Suzuki, PTEP **2013**, 083B03 (2013), arXiv:1304.0533 [hep-lat].
- [129] C. Monahan and K. Orginos, PoS **Lattice2013**, 443 (2013), arXiv:1311.2310 [hep-lat].
- [130] M. Lüscher, JHEP **1406**, 105 (2014), arXiv:1404.5930 [hep-lat].
- [131] T. Endo, K. Hieda, D. Miura, and H. Suzuki, PTEP **2015**, 053B03 (2015), arXiv:1502.01809 [hep-lat].
- [132] C. Monahan and K. Orginos, Phys. Rev. **D91**, 074513 (2015), arXiv:1501.05348 [hep-lat].
- [133] C. Monahan and K. Orginos, (2016), arXiv:1612.01584 [hep-lat].
- [134] M. Lüscher, JHEP **1008**, 071 (2010), arXiv:1006.4518 [hep-lat].
- [135] R. Lohmayer and H. Neuberger, PoS **LATTICE2011**, 249 (2011), arXiv:1110.3522 [hep-lat].
- [136] S. Syritsyn and J. W. Negele, *Proceedings, 25th International Symposium on Lattice field theory (Lattice 2007): Regensburg, Germany, July 30-August 4, 2007*, PoS **LAT2007**, 078 (2007), arXiv:0710.0425 [hep-lat].
- [137] A. Nicholson, E. Berkowitz, C. C. Chang, M. A. Clark, B. Joo, T. Kurth, E. Rinaldi, B. Tiburzi, P. Vranas, and A. Walker-Loud, in *Proceedings, 34th International Symposium on Lattice Field Theory (Lattice 2016): Southampton, UK, July 24-30, 2016* (2016) arXiv:1608.04793 [hep-lat].
- [138] C. Bouchard, C. C. Chang, T. Kurth, K. Orginos, and A. Walker-Loud, (2016), arXiv:1612.06963 [hep-lat].
- [139] T. Blum *et al.*, Phys. Rev. **D69**, 074502 (2004), arXiv:hep-lat/0007038 [hep-lat].
- [140] Y. Aoki *et al.*, Phys. Rev. **D69**, 074504 (2004), arXiv:hep-lat/0211023 [hep-lat].
- [141] S. Borsanyi *et al.*, JHEP **09**, 010 (2012), arXiv:1203.4469 [hep-lat].
- [142] A. Bazavov *et al.* (MILC), Phys. Rev. **D93**, 094510 (2016), arXiv:1503.02769 [hep-lat].
- [143] M. Albanese *et al.* (APE), Phys. Lett. **B192**, 163 (1987).
- [144] C. Bernard, S. Datta, T. A. DeGrand, C. E. DeTar, S. A. Gottlieb, U. M. Heller, C. McNeile, K. Orginos, R. Sugar, and D. Toussaint (MILC), Phys. Rev. **D66**, 094501 (2002), arXiv:hep-lat/0206016 [hep-lat].
- [145] A. Frommer, B. Nockel, S. Gusken, T. Lippert, and K. Schilling, Int. J. Mod. Phys. **C6**, 627 (1995), arXiv:hep-lat/9504020 [hep-lat].
- [146] H.-J. Kim and T. Izubuchi, *Proceedings, 31st International Symposium on Lattice Field Theory (Lattice 2013): Mainz, Germany, July 29-August 3, 2013*, PoS **LATTICE2013**, 033 (2014).
- [147] M. Clark, R. Babich, K. Barros, R. Brower, and C. Rebbi, Comput.Phys.Commun. **181**, 1517 (2010), arXiv:0911.3191 [hep-lat].
- [148] R. Babich, M. Clark, B. Joo, G. Shi, R. Brower, *et al.*, (2011), arXiv:1109.2935 [hep-lat].
- [149] T. Blum, T. Izubuchi, and C. Jung, *private communication*.
- [150] The HDF Group, “Hierarchical Data Format, version 5,” (1997-NNNN), <http://www.hdfgroup.org/HDF5/>.
- [151] T. Kurth, A. Pochinsky, A. Sarje, S. Syritsyn, and A. Walker-Loud, *Proceedings, 32nd International Symposium on Lattice Field Theory (Lattice 2014): Brookhaven, NY, USA, June 23-28, 2014*, PoS **LATTICE2014**, 045 (2015), arXiv:1501.06992 [hep-lat].
- [152] E. Berkowitz, “**METAQ**,” <https://github.com/evanberkowitz/metaq> (2016).
- [153] C. M. Bouchard, G. P. Lepage, C. Monahan, H. Na, and J. Shigemitsu, Phys. Rev. **D90**, 054506 (2014), arXiv:1406.2279 [hep-lat].
- [154] G. P. Lepage, “**lsqfit v8.1**,” (2016).